THE JOURNAL OF PHYSICAL CHEMISTRY B

 VOLUME 108, NUMBER 33, AUGUST 19, 2004

LETTERS

Toward the Solution Synthesis of the Tetrahedral Au_{20} Cluster

Hai-Feng Zhang,[†,‡] Matthias Stender,[†] Rui Zhang,[†] Chongmin Wang,[†] Jun Li,[*,†] and Lai-Sheng Wang[*,†,‡]

W. R. Wiley Environmental Molecular Sciences Laboratory, Pacific Northwest National Laboratory, P.O. Box 999, Richland, Washington 99352, and Department of Physics, Washington State University, 2710 University Drive, Richland, Washington 99352

Received: March 28, 2004; In Final Form: April 27, 2004

We report the observation in solution of the recently discovered tetrahedral Au_{20} cluster coordinated with eight PPh_3 (Ph = phenyl) ligands. The composition and molecular weight of the $Au_{20}(PPh_3)_8$ complex were confirmed by the isotopic pattern and accurate mass measurement of its doubly charged cation using high-resolution mass spectrometry. A collision-induced dissociation experiment showed that four PPh_3 ligands can be easily removed from $Au_{20}(PPh_3)_8^{2+}$, resulting in a highly stable $Au_{20}(PPh_3)_4^{2+}$ ion. This observation is consistent with the tetrahedral Au_{20}, in which the four apex sites are expected to bond to the PPh_3 ligands strongly, and is confirmed by theoretical calculations that predict a highly stable $Au_{20}(PH_3)_4$ complex with $Au-PH_3$ bond energies of ~1 eV. The current experimental and theoretical observations suggest that large quantities of ligand-stabilized tetrahedral Au_{20} can be obtained, opening the door for exploring its anticipated novel chemical, optical, and catalytic properties.

One of the longstanding objectives of cluster science is to discover highly stable clusters and use them as building blocks for bulk cluster-assembled materials. The discovery of C_{60} in the gas phase[1] and its subsequent bulk synthesis[2] provide classical inspiration and a prototypical example. However, it is generally believed that few other stable gaseous clusters may be assembled into bulk materials because of cluster−cluster interactions leading to agglomeration. Indeed, no cluster-assembled materials have been synthesized on the basis of stable gaseous clusters other than the fullerenes, despite intensive experimental and theoretical efforts.[3−9] Recently, we reported that a 20-atom gold cluster possesses a tetrahedral (T_d) structure with a remarkably large HOMO−LUMO energy gap, suggesting that it would be highly chemically inert and may have novel optical and catalytic properties.[10] Here we report the observation of the tetrahedral Au_{20} cluster in solution, ligated with triphenyl phosphine (PPh_3) ligands, and its confirmation by theoretical calculations. The current work represents a successful synthetic effort directly guided and motivated by a gas-phase observation, validating the gas-phase-to-condensed-phase approach for the discovery of cluster-assembled nanomaterials.

There has been a long history of investigations on gold nanoparticles.[11] Recent interest has been stimulated by the discovery of catalytic effects in supported gold nanoparticles[12−15] and the potential applications of gold nanoparticles in nanoelectronics and nanobiology.[16−22] Gold nanoparticles are generally synthesized in solution with closely packed thiol ligands on their surfaces as a protection layer.[11,23] The smallest thiol-protected gold nanoparticles are ~0.9 nm in diameter and are proposed to contain 28 Au atoms.[24] Many small multinuclear gold clusters with PPh_3 ligands have been synthesized and characterized crystallographically.[25] The largest structurally

* To whom correspondence should be addressed. E-mail: jun.li@pnl.gov or ls.wang@pnl.gov.
[†] Pacific Northwest National Laboratory.
[‡] Washington State University.

10.1021/jp048636q CCC: $27.50
Published on Web 05/19/2004

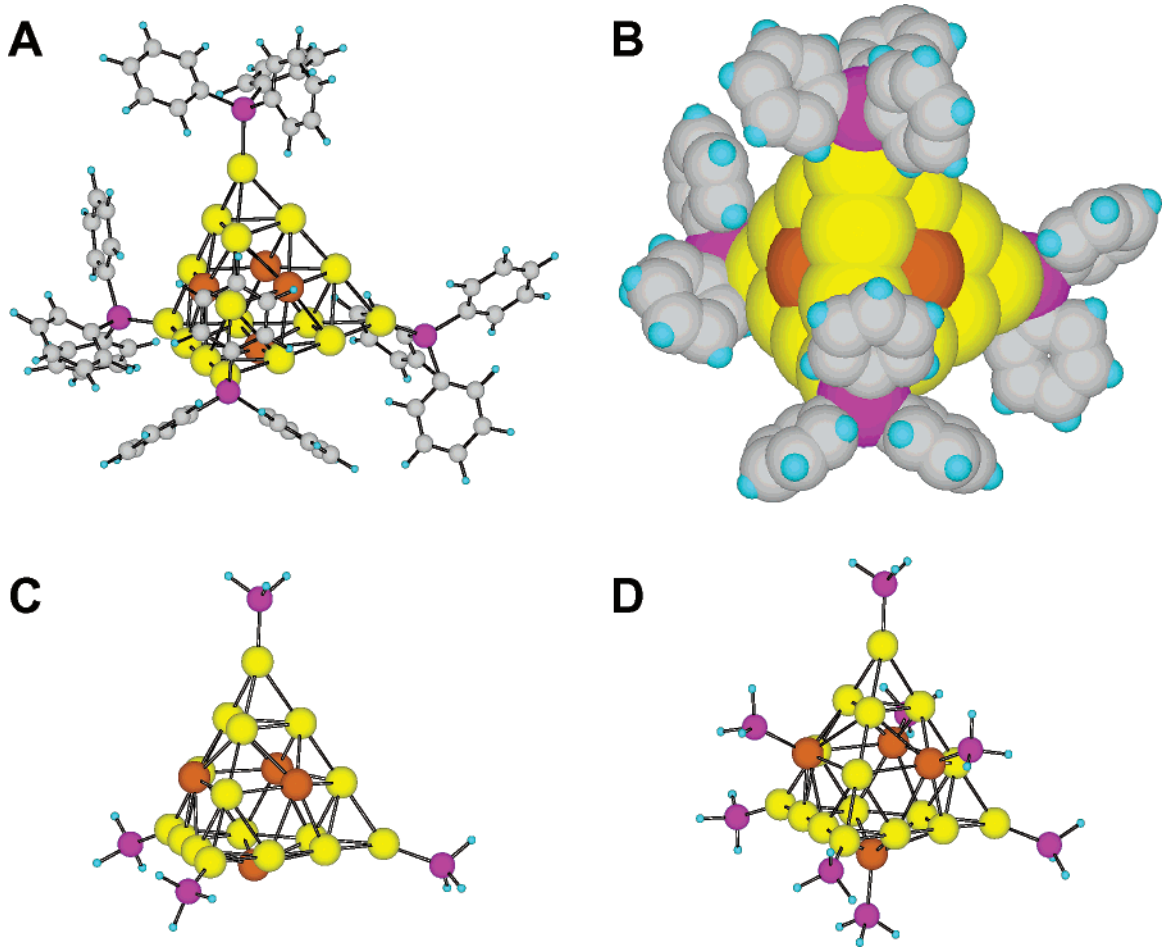

Figure 1. Computed structures of Au_{20} and its phosphine complexes.[31] (A) $Au_{20}(PPh_3)_4$. (B) van der Waals surface of $Au_{20}(PPh_3)_4$. (C) $Au_{20}(PH_3)_4$. (D) $Au_{20}(PH_3)_8$.

characterized gold clusters with PPh_3 ligands contain 13 and 39 atoms,[25−27] although a "greengold" compound has been identified and proposed to contain 75 Au atoms.[28] The tetrahedral Au_{20} occupies a unique position in the hierarchy of gold clusters and nanoparticles. There are no known PPh_3-coordinated gold clusters, nor are there known thiol-protected gold nanoparticles with a T_d Au_{20} core. The T_d structure of Au_{20} is highly unique; it can be viewed as a fragment of the bulk fcc lattice, but unlike the bulk crystal, it has a large energy gap.[10] It is also the largest metal cluster with close packing and yet with every atom on the surface.[29] The only other known transition-metal cluster compound that has been structurally characterized to have a 20-atom T_d core is $[Os_{20}(CO)_{40}]^{2-}$.[30]

Because of potential cluster−cluster agglomeration, Au_{20} must also be protected by ligands in order to use it as a building block for cluster-assembled materials. To maintain the unique structural and electronic properties of the T_d Au_{20}, the ligands have to be carefully chosen. The thiol ligands have strong chemical interactions with Au and would alter the electronic structure of the T_d Au_{20}. In addition, thiol ligands tend to form a close-packed monolayer on gold nanoparticles, leaving no atomic sites for catalysis. Thus, we chose the zero-valent PPh_3 ligands, which form only dative bonding to Au and offer the potential that both the T_d Au_{20} core and its unique electronic structure would not be destroyed. Inasmuch as the four apex sites of Au_{20} are more reactive, we reasoned that the bulky PPh_3 ligands may coordinate only to these sites, leaving 16 uncoordinated surface sites for chemisorption and catalysis. Preliminary theoretical calculations (Figure 1A−C) revealed that the $Au_{20}(PR_3)_4$ (R = H, Ph) complexes indeed possess high stability.[31] Figure 1A shows the optimized structure of Au_{20} coordinated with four PPh_3 ligands; its van der Waals surface is shown in Figure 1B. We also calculated $Au_{20}(PH_3)_4$ for computational simplicity (Figure 1C), expecting that the effect of PH_3 on the Au_{20} core would be similar to that of PPh_3. Indeed, the only effect that the phosphine ligands have on the Au_{20} core is that the four face-centered Au atoms tend to be pushed outward from the four Au_{10} faces: the calculated distance between the face-centered atoms is increased from 3.1 Å in Au_{20} to 3.4 Å (4.0 Å) in $Au_{20}(PPh_3)_4$ [$Au_{20}(PH_3)_4$]. But the ligated complexes still maintain a large HOMO−LUMO energy gap: 1.44 eV in $Au_{20}(PPh_3)_4$ and 1.82 eV in $Au_{20}(PH_3)_4$, compared to 1.77 eV in the parent Au_{20}.[10]

We started our synthesis of PPh_3-protected Au_{20} using a two-phase system similar to that used in the literature for the synthesis of small phosphine-stabilized gold nanoparticles.[32,33] $AuCl(PPh_3)$ (1.482 g, 3 mmol) and tetraoctylammonium bromide (1.803 g, 3.3 mmol) were dissolved in a toluene/water mixture (200 mL/150 mL). After ca. 15 min, 1.134 g (30 mmol) of $NaBH_4$ dissolved in 25 mL of water was added dropwise via cannula under vigorous stirring. The reaction mixture turned dark brown instantly under bubbling. The reaction was stirred overnight. The organic phase was separated from the aqueous layer and washed with water (2 × 200 mL). The toluene was removed in vacuo under gentle heating (60 °C). The resulting black solid was dissolved in dichloromethane and precipitated by the slow addition of pentane. The solid was filtered and washed several times with hexanes (3 × 100 mL), a 1:1

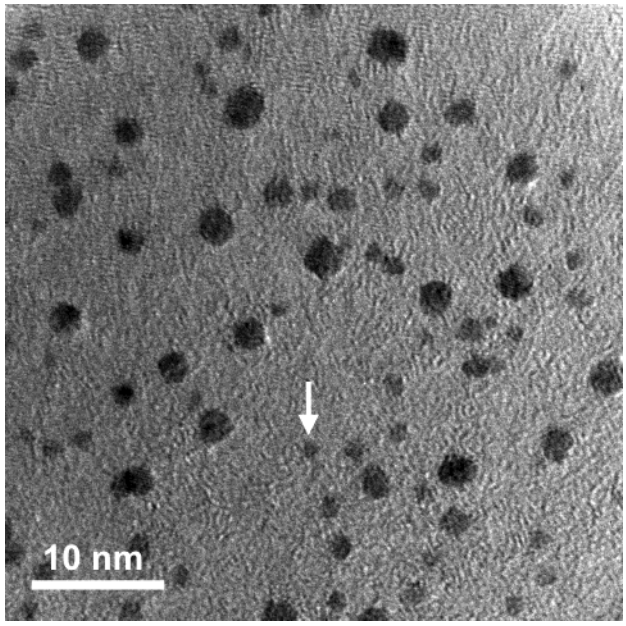

Figure 2. High-resolution transmission electron microscopy image of the synthesized Au−phosphine nanoparticles. The arrow points to one possible Au_{20} cluster. HRTEM analysis was carried out on a JEOL JEM 2010 microscope fitted with a LaB_6 filament and a specified point-to-point resolution of 0.194 nm. The operating voltage of the microscope was 200 kV. The image was digitally recorded with a slow-scan CCD camera (image size 1024 × 1024 pixels, Digital Micrograph software from Gatan, Pleasant, CA).

methanol/water mixture (3 × 100 mL), diethyl ether (50 mL), and pentane (2 × 50 mL). The final product was dried in vacuo with a yield of 507 mg.

A small portion of the solid sample was dissolved in an ethanol/CH_2Cl_2 mixed solvent (10:1 volume ratio), which was centrifuged to remove the large particles. The solution turned from dark to brownish after the centrifugation. A drop of the brownish solution was spread onto an amorphous carbon-coated copper grid and dried in preparation for high-resolution transmission electron microscopy (HRTEM). The HRTEM image (Figure 2) showed that the soluble samples contained gold nanoparticles with diameters as large as 3 nm, but the majority of the particles have diameters of less than 1 nm. Each edge of the bare Au_{20} was calculated to be 0.81 nm and was not changed in the PH_3-capped complex. Thus, the T_d Au_{20} core is expected to give a triangular image with edges slightly less than 1 nm. Indeed, numerous triangular particles with dimensions of less than 1 nm can be found in the TEM image, consistent with the anticipated PPh_3-capped Au_{20}.

We further characterized the sample using a high-resolution Fourier transform ion cyclotron resonance (FTICR) mass spectrometer, which was accurately calibrated and equipped with an electrospray ionization (ESI) source.[34] The solution sample was introduced into the ESI ion source through direct infusion using a syringe pump. The mass analysis was carried out in both positive and negative ion modes. Mass scans were optimized for different mass-to-charge (m/z) ranges from 1000 up to more than 10 000. Very high m/z ions (>5000) were observed, most likely corresponding to those gold clusters of more than 1 nm in diameter (Figure 2). We carefully searched the m/z range around $Au_{20}(PPh_3)_4^+$ (m/z = 4987.695) but did not observe any singly charged ions in this mass range. All of the mass peaks observed in this m/z range and in higher m/z ranges appeared to be doubly charged ions, which could be easily recognized from the $^1/_2$ m/z difference in the isotopic

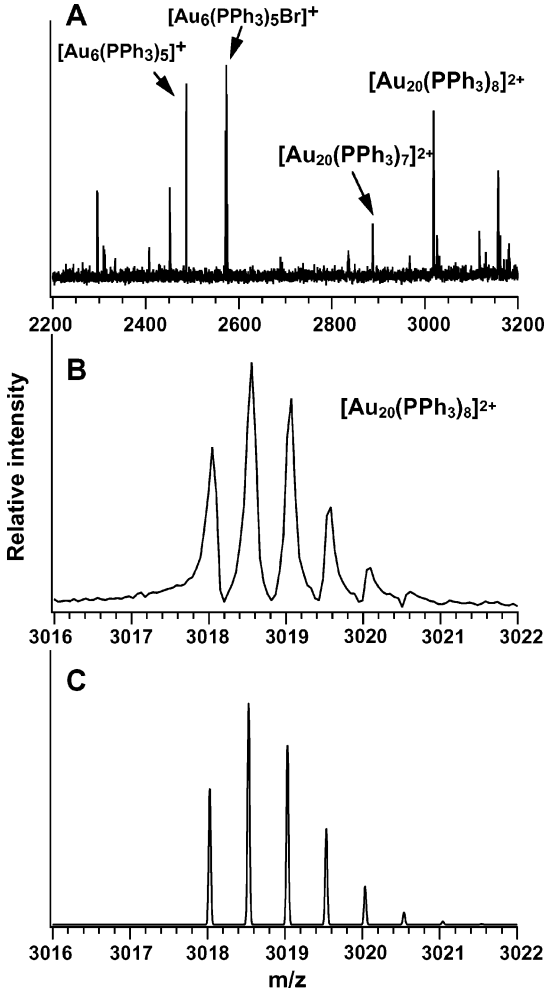

Figure 3. High-resolution mass spectroscopic characterization of Au−PPh_3 complexes. (A) Mass spectrum containing the $Au_{20}(PPh_3)_8^{2+}$ and $Au_{20}(PPh_3)_7^{2+}$ doubly charged clusters. (B) Isotopic pattern of the $Au_{20}(PPh_3)_8^{2+}$ mass peak. (C) Simulated isotopic pattern using the natural isotopic abundances of Au, P, C, and H.

patterns. We then searched the lower m/z range corresponding to $Au_{20}(PPh_3)_4^{2+}$ (m/z = 2493.848), as shown in Figure 3A. Prominent singly charged ions were observed, corresponding to five- and six-atom gold clusters, but no doubly charged ions at m/z = 2493.848 were observed. However, a careful examination of the mass spectrum revealed that doubly charged ions corresponding to Au_{20} clusters with eight and seven PPh_3 ligands were observed at m/z = 3018.030 and 2886.984, respectively. We also observed mass peaks corresponding to Au_{10} complexes, but familiar clusters such as the undecanuclear Au_{11} species were not observed under our experimental conditions.

Figure 3B shows the observed isotopic pattern of the $Au_{20}(PPh_3)_8^{2+}$ cation primarily due to the ^{13}C isotope, compared to the simulated isotopic pattern (Figure 3C). The perfect agreement between the experimental and the simulated isotopic patterns, as well as the accurate m/z measurement, unequivocally confirmed the correct identification of the composition of the $Au_{20}(PPh_3)_8^{2+}$ cluster. Such good agreement was also obtained for the observed $Au_{20}(PPh_3)_7^{2+}$ ions. To obtain structural information for the $Au_{20}(PPh_3)_8^{2+}$ cluster, we conducted collision-induced dissociation (CID) experiments in the FTICR cell. The $Au_{20}(PPh_3)_8^{2+}$ ions were first isolated from a broadband detection (Figure 4A) and then excited to collide with background gas molecules (10^{-7} Torr of benzene in this case). The excitation method used was the so-called sustained off-resonance

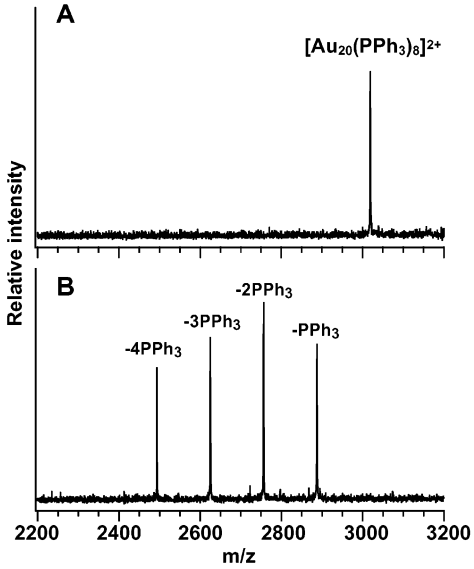

Figure 4. Collision-induced dissociation (CID) of $Au_{20}(PPh_3)_8^{2+}$. (A) $Au_{20}(PPh_3)_8^{2+}$ peak after mass isolation. (B) SORI-CID of $Au_{20}(PPh_3)_8^{2+}$.[35−37] Parent $Au_{20}(PPh_3)_8^{2+}$ ions were excited with a 1000-Hz frequency offset, which provided an average collision energy of ∼0.64 eV. The collision gas (benzene) was pulsed into the ICR cell, reaching a peak pressure at 1×10^{-7} Torr. The product ions, $Au_{20}(PPh_3)_x^{2+}$, were terminated at $x = 4$, and no more PPh_3 could be removed under the current CID condition.

irradiation (SORI),[35] which has proven to be more efficient for the dissociation of large molecules such as large peptides and proteins.[36] The CID experiment (Figure 4B) revealed that four PPh_3 ligands can be readily dissociated from $Au_{20}(PPh_3)_8^{2+}$, resulting in a highly stable $Au_{20}(PPh_3)_4^{2+}$ cluster ion, which could not be dissociated further under our current experimental conditions.[37]

The CID results suggested that the tetrahedral core of Au_{20} is intact in the PPh_3-coordinated clusters, which is consistent with our initial expectation and calculation that the four apex sites of Au_{20} are the most reactive sites that bind strongly to the four PPh_3 ligands. We further computed a Au_{20} cluster coordinated by eight PH_3 (Figure 1D), with the four additional PH_3 ligands coordinated to the face-centered sites.[31] Our calculations showed that the T_d Au_{20} core is intact in $Au_{20}(PH_3)_8$, which also has a large energy gap (1.55 eV) that is only slightly smaller than that of Au_{20}. The edge length of the T_d Au_{20} was not influenced by the PH_3 coordination; the only structural change is the outward move of the face-centered atoms. The four face-centered atoms in Au_{20} form a smaller tetrahedron, with a Au−Au distance of 3.1 Å that is increased to 4.0 Å in $Au_{20}(PH_3)_4$ and 4.7 Å in $Au_{20}(PH_3)_8$. The average binding energy of PH_3 to the face-centered sites was calculated to be 16 kcal/mol, which is still sizable but smaller than that of the apex sites. We should point out that the Au−PPh_3 binding energy is expected to be larger for the apex sites and smaller for the face-centered sites because of steric repulsion between the bulkier PPh_3 ligands compared to that of the PH_3 ligands used in the calculations. Thus, our theoretical results were completely consistent with the CID experiment and confirmed that the T_d Au_{20} core is a robust cluster building block.

The phosphine ligands are electron donors, causing the increase in the HOMO energies of Au_{20} from −5.60 eV in the bare cluster to −4.51 eV in $Au_{20}(PH_3)_4$ and −3.89 eV in $Au_{20}(PH_3)_8$. This result suggests that the latter has a relatively low ionization energy and may exist as doubly charged closed-shell cations in solution.[38] This explains why we were not able to observe singly charged $Au_{20}(PPh_3)_8^{+}$ from the ESI source. It also explains why we did not observe negatively charged $Au_{20}(PPh_3)_8^{-}$ ions when the negative mode was used in the ESI.[39] The weaker $Au_{20}(PPh_3)_7^{2+}$ ion signals may be produced from the dissociation of the parent $Au_{20}(PPh_3)_8^{2+}$ in the ESI source. The current experimental and theoretical results suggest that the T_d Au_{20} cluster coordinated with phosphine ligands may be obtained in bulk quantity. It is expected that by increasing the size of the ligands one can synthesize the T_d Au_{20} clusters with only the four apex sites coordinated. These clusters may be promising catalysts with the highest surface area and well-defined surface sites.

Acknowledgment. This work was supported by the National Science Foundation (CHE-0349426 to L.-S.W.) and performed at the EMSL, a national scientific user facility sponsored by DOE's Office of Biological and Environmental Research and located at the Pacific Northwest National Laboratory, operated for DOE by Battelle. All calculations were performed using supercomputers at EMSL MSCF.

References and Notes

(1) Kroto, H. W.; Heath, J. R.; O'Brien, S. C.; Curl, R. F.; Smalley, R. E. *Nature* **1985**, *318*, 162.
(2) Krätschmer, W.; Lamb, L. D.; Fostiropoulos, K.; Huffman, D. R. *Nature* **1990**, *347*, 354.
(3) Guo, B. C.; Kerns, K. P.; Castleman, A. W., Jr. *Science* **1992**, *255*, 1411.
(4) Khanna, S. N.; Jena, P. *Phys. Rev. Lett.* **1992**, *169*, 664.
(5) Gong, X. G.; Kumar, V. *Phys. Rev. Lett.* **1993**, *70*, 2078.
(6) Hiura, H.; Miyazaki, T.; Kanayama, T. *Phys. Rev. Lett.* **2001**, *86*, 1733.
(7) Nakajima, A.; Kaya, K. *J. Phys. Chem. A* **2000**, *104*, 176.
(8) Thomas, O. C.; Zheng, W.; Bowen, K. H., Jr. *J. Chem. Phys.* **2001**, *114*, 5514.
(9) Grass, M.; Fischer, D.; Mathes, M.; Gantefor, G.; Nielaba, P. *Appl. Phys. Lett.* **2002**, *81*, 3810.
(10) Li, J.; Li, X.; Zhai, H. J.; Wang, L. S. *Science* **2003**, *299*, 864.
(11) See an excellent recent review: Daniel, M. C.; Astruc, D. *Chem. Rev.* **2004**, *104*, 293.
(12) Haruta, M. *Catal. Today* **1997**, *36*, 153.
(13) Valden, M.; Lai, X.; Goodman, D. W. *Science* **1998**, *281*, 1647.
(14) Heiz, U.; Schneider, W. D. *J. Phys. D: Appl. Phys.* **2000**, *33*, R85.
(15) Sanchez, A.; Abbet, S.; Heiz, U.; Schneider, W.-D.; Häkkinen, H.; Barnett, R. N.; Landman, U. *J. Phys. Chem. A* **1999**, *103*, 9573.
(16) Gittins, D. I.; Bethell, D.; Schiffrin, D. J.; Nichols, R. J. *Nature* **2000**, *408*, 67.
(17) Whetten, R. L.; Shafigullin, M. N.; Khoury, J. T.; Schaaff, T. G.; Vezmar, I.; Alvarez, M. M.; Wilkinson, A. *Acc. Chem. Res.* **1999**, *32*, 397.
(18) Templeton, A. C.; Wuelfing, W. P.; Murray, R. W. *Acc. Chem. Res.* **2000**, *33*, 27.
(19) Luedtke, W. D.; Landman, U. *J. Phys. Chem.* **1996**, *100*, 13323.
(20) Schmid, G.; Corain, B. *Eur. J. Inorg. Chem.* **2003**, 3081.
(21) Schwerdtfeger, P. *Angew. Chem., Int. Ed.* **2003**, *42*, 1892.
(22) Elghanian, R.; Storhoff, J. J.; Mucic, R. C.; Letsinger, R. L.; Mirkin, C. A. *Science* **1997**, *277*, 1078.
(23) Brust, M.; Walker, M.; Bethell, D.; Schiffrin, D. J.; Whyman, R. *J. Chem. Soc., Chem. Commun.* **1994**, 801.
(24) Schaaff, T. G.; Knight, G.; Shafigullin, M. N.; Borkman, R. F.; Whetten, R. L. *J. Phys. Chem. B* **1998**, *102*, 10643.
(25) Hall, K. P.; Mingos, D. M. P. *Prog. Inorg. Chem.* **1985**, 237.
(26) Briant, C. E.; Theobald, B. R. C.; White, J. W.; Bell, L. K.; Mingos, D. M. P. *J. Chem. Soc., Chem. Commun.* **1981**, 201.
(27) Teo, B. K.; Shi, X.; Zhang, H. *J. Am. Chem. Soc.* **1992**, *114*, 2743.
(28) Gutiérrez, E.; Powell, R. D.; Furuya, F. R.; Hainfeld, J. F.; Schaaff, T. G.; Shafigullin, M. N.; Stephens, P. W.; Whetten, R. L. *Eur. Phys. J. D* **1999**, *9*, 647.
(29) Mingos, D. M. P.; Slee, T.; Lin, Z. *Chem. Rev.* **1990**, *90*, 383.
(30) Gade, L. H.; Johnson, B. F. G.; Lewis, J.; McPartlin, M.; Powell, H. R.; Raithby, P. R.; Wong, W. T. *J. Chem. Soc., Dalton Trans.* **1994**, 521.
(31) The Au_{20}−phosphine clusters were calculated via relativistic density functional theory using the ADF 2003 code [*ADF 2003.01*, SCM, Theoretical Chemistry, Vrije Universiteit: Amsterdam, The Netherlands (http://www.scm.com)]. All geometries were fully optimized by using an

analytical energy gradient technique without imposing any symmetry restrictions. The gradient-corrected PW91 exchange-correlation functional was used in the electronic structure calculations and geometry optimizations (Perdew, J. P.; Wang, Y. *Phys. Rev. B* **1992**, *45*, 13244). The scalar relativistic effects were taken into account via the zero-order-regular approximation (ZORA) (Lenthe, E. Van; Baerends, E. J.; Snijders, J. G. *J. Chem. Phys.* **1993**, *99*, 4597). Spin−orbit coupling effects were evaluated on the basis of single-point calculations performed at the optimized scalar relativistic structures. The Slater-type-orbit (STO) basis sets with triple-ζ plus two polarization functions (TZ2P) quality were used for Au and P atoms, with basis sets of double-ζ plus one polarization function (DZP) for C and H atoms (Lenthe, E. Van; Baerends, E. J. *J. Comput. Chem*. **2003**, *24*, 1142). The frozen-core approximation was applied to the [$1s^2$] cores of C, [$1s^2-2p^6$] core of P, and [$1s^2-4f^{14}$] core of Au (Baerends, E. J.; Ellis, D. E.; Ros, P. *Chem. Phys*. **1973**, *2*, 42).

(32) Weare, W. W.; Reed, S. M.; Warner, M. G.; Hutchison, J. E. *J. Am. Chem. Soc*. **2000**, *122*, 12890.

(33) All reagents used in the synthesis were commercially available. Chlorotriphenylphospine gold(I) was purchased from Strem Chemicals; tetraoctylammonium bromide, from Fluka; and sodium borohydride, from Aldrich. Toluene was purchased from Aldrich and was packed under nitrogen in a Sure/Seal bottle. Deionized water was used in the reaction and in the subsequent washes. The water was sparged with argon. All reagents were used as received without further purification. All manipulations were carried out under an atmosphere of argon using standard Schlenk and cannula techniques.

(34) The mass spectrometry analysis of the $Au_{20}-PPh_3$ clusters was carried out on an FTICR mass spectrometer equipped with a 9.4-T superconducting magnet. This instrument was manufactured by Bruker Daltonics (Billerica, MA), and it is the latest model in the BioAPEX series (APEX-Q), which has an Apollo ESI source and a quadrupole/hexapole interface to allow external ion generation, selection, and fragmentation. The instrument was mass calibrated prior to sample analysis using a Hewlett-Packard calibration mixture (Flanagan, J. M. U.S. Patent 5,872,357, 1999). The average mass measurement error in the mass range up to *m*/*z* 4000 was <2 ppm. The mass spectral data were acquired using a 1-MB data set, and the peak resolution ($\Delta M/M$) at *m*/*z* 1000 exceeded 100 000. At such high resolution, the isotopic information of the analyte ions was totally resolved.

(35) Heck, A. J. R.; Koning, L. J. de; Pinkse, F. A.; Nibbering, M. M. *Rapid Commum. Mass Spectrom.* **1991**, *5*, 406.

(36) Hettich, R. L.; Stemmler, E. A. *Rapid Commun. Mass Spectrom.* **1996**, *10*, 321.

(37) The average collision energy for SORI-CID could be calculated using an equation introduced by Marshall's group. See Huang, Y. L.; Pasa-Tolic, L.; Guan, S. H.; Marshall, A. G. *Anal. Chem.* **1994**, *66*, 4385. For the CID experiment performed with $Au_{20}(PPh_3)_8^{2+}$, the estimated average energy was ~0.64 eV.

(38) The HOMO of T_d Au_{20} is doubly degenerate.[10] However, in $Au_{20}(PPh_3)_8$ the total molecular symmetry is lowered, even though the Au_{20} core still maintains its local T_d symmetry. Thus, the HOMO degeneracy is lifted in $Au_{20}(PPh_3)_8$, leading to a closed-shell dication when two electrons are removed from $Au_{20}(PPh_3)_8$. It should be noted that in the dication the Au_{20} core possesses only 18 valence electrons, which is also a major shell closing in the electron shell model, supporting the viability of the dication. We also optimized the structure of the $Au_{20}(PPh_3)_8^{2+}$ dication theoretically and confirmed its stability. Our preliminary calculations showed that the structure of the dication is very similar to that of the neutral.

(39) In the negative-ion mode, only a few low-intensity singly charged anions below *m*/*z* 2500 were observed. The *m*/*z* values and the isotope distributions of these ions indicated that they were very small Au-containing clusters with fragmented ligands most likely due to extensive dissociations from larger and positively charged parent clusters during electrospray.